

# RADAR EQUATIONS

for **Modern  
Radar**

 DVD  
INCLUDED



David K. Barton

# **Radar Equations for Modern Radar**

## DISCLAIMER OF WARRANTY

The technical descriptions, procedures, and computer programs in this book have been developed with the greatest of care and they have been useful to the author in a broad range of applications; however, they are provided as is, without warranty of any kind. Artech House and the author and editors of the book titled *Radar Equations for Modern Radar* make no warranties, expressed or implied, that the equations, programs, and procedures in this book or its associated software are free of error, or are consistent with any particular standard of merchantability, or will meet your requirements for any particular application. They should not be relied upon for solving a problem whose incorrect solution could result in injury to a person or loss of property. Any use of the programs or procedures in such a manner is at the user's own risk. The editors, author, and publisher disclaim all liability for direct, incidental, or consequent damages resulting from use of the programs or procedures in this book or the associated software.

For a complete listing of titles in the  
*Artech House Radar Series*,  
turn to the back of this book.

# **Radar Equations for Modern Radar**

David K. Barton



**ARTECH  
HOUSE**

BOSTON | LONDON  
[artechhouse.com](http://artechhouse.com)

**Library of Congress Cataloging-in-Publication Data**

A catalog record for this book is available from the U.S. Library of Congress.

**British Library Cataloguing in Publication Data**

A catalogue record for this book is available from the British Library.

**Cover design by Vicki Kane**

ISBN 13: 978-1-60807-521-8

© 2013 ARTECH HOUSE

685 Canton Street

Norwood, MA 02062

All rights reserved. Printed and bound in the United States of America. No part of this book may be reproduced or utilized in any form or by any means, electronic or mechanical, including photocopying, recording, or by any information storage and retrieval system, without permission in writing from the publisher.

All terms mentioned in this book that are known to be trademarks or service marks have been appropriately capitalized. Artech House cannot attest to the accuracy of this information. Use of a term in this book should not be regarded as affecting the validity of any trademark or service mark.

10 9 8 7 6 5 4 3 2 1

# Contents

Preface . . . . .	xv
Chapter 1 Development of the Radar Equation . . . . .	1
1.1 Radar Equation Fundamentals . . . . .	1
1.1.1 Maximum Available Signal-to-Noise Ratio . . . . .	2
1.1.2 Minimum Required Signal-to-Noise Ratio . . . . .	4
1.1.3 Maximum Detection Range for Pulsed Radar . . . . .	5
1.2 The Original Radar Equation . . . . .	5
1.3 Blake's Radar Equation for Pulsed Radar . . . . .	6
1.3.1 Significance of Terms in Blake's Equation . . . . .	7
1.3.2 Methods of Solving for Range . . . . .	9
1.3.3 Advantages of the Blake Chart . . . . .	11
1.3.4 Blake's Coherent Radar Equation . . . . .	11
1.3.5 Blake's Bistatic Range Equation . . . . .	12
1.4 Other Forms of the Radar Equation . . . . .	13
1.4.1 Hall's Radar Equations . . . . .	13
1.4.2 Barton's Radar Equations . . . . .	14
1.5 Avoiding Pitfalls in Range Calculation . . . . .	16
1.5.1 System Noise Temperature $T_s$ . . . . .	16
1.5.2 Use of Signal-to-Noise Energy Ratio . . . . .	17
1.5.3 Use of Average Power . . . . .	18
1.5.4 Bandwidth Correction and Matching Factors . . . . .	18
1.5.5 Detectability Factors for Arbitrary Targets . . . . .	18
1.5.6 Pattern-Propagation Factor . . . . .	19
1.5.7 Loss Factors . . . . .	19
1.5.8 Summary of Pitfalls in Range Calculation . . . . .	20
1.6 Radar Equation for Modern Radar Systems . . . . .	20
1.6.1 Factors Requiring Modifications to the Radar Equation . . . . .	20
1.6.2 Equations Applicable to Modern Radars . . . . .	23
1.6.3 Method of Calculating Detection Range . . . . .	24
1.6.4 Vertical Coverage Charts . . . . .	27
1.6.5 Required Probability of Detection . . . . .	28

	1.7	Summary of Radar Equation Development . . . . .	30
		References . . . . .	30
Chapter 2		The Search Radar Equation . . . . .	33
	2.1	Derivation of the Search Radar Equation . . . . .	34
	2.2	Search Sectors for Air Surveillance . . . . .	37
	2.2.1	Elevation Coverage in 2-D Surveillance . . . . .	37
	2.2.2	Fan-Beam Pattern for 2-D Air Surveillance . . . . .	38
	2.2.3	Cosecant-Squared Pattern for 2-D Surveillance . . . . .	39
	2.2.4	Coverage to Constant Altitude . . . . .	40
	2.2.5	Enhanced Upper Coverage for 2-D Surveillance . . . . .	40
	2.2.6	Reflector Antenna design for 2-D Surveillance Radar . . . . .	41
	2.2.7	Array Antennas for 2-D Surveillance Radar . . . . .	41
	2.2.8	Example of Required Power-Aperture Product for 2-D Radar . . . . .	42
	2.3	Three-Dimensional Air Surveillance . . . . .	43
	2.3.1	Stacked-Beam 3-D Surveillance Radar . . . . .	43
	2.3.2	Scanning-beam 3-D Surveillance Radars . . . . .	43
	2.3.3	Search Losses for 3-D Surveillance Radar . . . . .	44
	2.4	Surveillance with Multifunction Array Radar . . . . .	44
	2.4.1	Example of MFAR Search Sectors . . . . .	45
	2.4.2	Advantages and Disadvantages of MFAR Search . . . . .	46
	2.4.3	Example of Search Radar Equation for MFAR . . . . .	47
	2.5	The Search Fence . . . . .	48
	2.5.1	Search Sector for the Fence . . . . .	49
	2.5.2	Example ICBM Fence . . . . .	50
	2.6	Search Losses . . . . .	51
	2.6.1	Reduction in Available Energy Ratio . . . . .	51
	2.6.2	Increase in Required Energy Ratio . . . . .	52
	2.6.3	Summary of Losses . . . . .	52
		References . . . . .	54
Chapter 3		Radar Equations for Clutter and Jamming . . . . .	55
	3.1	Signal-to-Interference Ratio . . . . .	55
	3.2	Clutter Effect on Detection Range . . . . .	57
	3.2.1	Range-Ambiguous Clutter . . . . .	57
	3.2.2	Types of Radar Waveforms . . . . .	58
	3.2.3	Clutter Detectability Factor . . . . .	59
	3.2.4	Effective Spectral Density of Clutter . . . . .	61
	3.2.5	Detection Range with Clutter . . . . .	62

3.3	Detection in Surface Clutter . . . . .	62
3.3.1	Clutter from a Flat Surface . . . . .	62
3.3.2	Surface Clutter from the Spherical Earth . . . . .	65
3.3.3	Surface Clutter Cross Section . . . . .	66
3.3.4	Input Energy of Surface Clutter . . . . .	68
3.3.5	Detection Range of Surface-Based CW and HPRF Radars . . . . .	73
3.3.6	Summary of Detection in Surface Clutter . . . . .	76
3.4	Detection in Volume Clutter . . . . .	77
3.4.1	Geometry of Volume Clutter . . . . .	77
3.4.2	Volume Clutter Cross Section . . . . .	78
3.4.3	Volume Clutter Energy . . . . .	79
3.4.4	Volume Clutter Detectability Factor . . . . .	80
3.4.5	Detection Range in Volume Clutter and Noise . . . . .	80
3.4.6	Volume Clutter in CW and PD Radars . . . . .	82
3.4.7	Summary of Detection in Volume Clutter . . . . .	87
3.5	Effects of Discrete Clutter . . . . .	88
3.5.1	Effect of False Alarms . . . . .	89
3.5.2	Required Noise False-Alarm Probability . . . . .	89
3.5.3	Requirements for Rejection of Discrete Clutter . . . . .	90
3.5.4	Summary of Discrete Clutter Effects . . . . .	91
3.6	Sidelobe Clutter . . . . .	91
3.6.1	Surface Clutter in Sidelobes . . . . .	91
3.6.2	Volume Clutter in Sidelobes . . . . .	93
3.7	Detection in Noise Jamming . . . . .	94
3.7.1	Objective and Methods of Noise Jamming . . . . .	94
3.7.2	Radar Equations for Noise Jamming . . . . .	96
3.7.3	Examples of Noise Jamming . . . . .	98
3.8	Deceptive Jamming . . . . .	101
3.8.1	Range Equations for Deceptive Jamming . . . . .	102
3.9	Summary of Detection in Jamming . . . . .	106
3.9.1	Range with Noise Jamming . . . . .	106
3.9.2	Deceptive Jammer Equations . . . . .	106
3.10	Detection in Combined Interference . . . . .	106
	References . . . . .	107

Chapter 4	Detection Theory . . . . .	109
4.1	Background . . . . .	109
4.2	Steady-Target Detectability Factor . . . . .	110
4.2.1	Exact Steady-Target Detection Probability . . . . .	111
4.2.2	Threshold Level . . . . .	111
4.2.3	Exact Steady-Target Detectability Factor . . . . .	114

	4.2.4	Exact Single-Pulse, Steady-Target Detectability Factor . . . . .	114
	4.2.5	Approximations for Single-Pulse, Steady-Target Detectability Factor . . . . .	115
	4.2.6	Approximations for $n$ -Pulse, Steady-Target Detectability Factor . . . . .	116
4.3		Detectability Factors for Fluctuating Targets . . . . .	118
	4.3.1	Generalized Chi-Square Target Fluctuation Model . . . . .	118
	4.3.2	Detection of Signals with Chi-Square Statistics	119
	4.3.3	Swerling Case 1 . . . . .	120
	4.3.4	Swerling Case 2 . . . . .	124
	4.3.5	Swerling Case 3 . . . . .	125
	4.3.6	Swerling Case 4 . . . . .	127
4.4		Equations Based on Detector Loss . . . . .	127
	4.4.1	Coherent Detection . . . . .	127
	4.4.2	Envelope Detection and Detector Loss . . . . .	129
	4.4.3	Integration Loss . . . . .	129
	4.4.4	Integration Gain . . . . .	131
	4.4.5	Fluctuation Loss . . . . .	132
	4.4.6	Case 1 Detectability Factor . . . . .	133
	4.4.7	Detectability Factors for Other Fluctuating Targets . . . . .	134
4.5		Diversity in Radar . . . . .	134
	4.5.1	Diversity Gain . . . . .	134
	4.5.2	Signal and Target Models with Diversity . . . . .	135
4.6		Visibility Factor . . . . .	138
4.7		Summary of Detection Theory . . . . .	140
		References . . . . .	141
Chapter 5		Beamshape Loss . . . . .	143
	5.1	Background . . . . .	143
		5.1.1 Definition of Beamshape Loss . . . . .	143
		5.1.2 Sampling in Angle Space . . . . .	144
		5.1.3 Literature on Beamshape Loss . . . . .	145
	5.2	Beamshape Loss with Dense Sampling . . . . .	146
		5.2.1 Simple Beamshape Loss Model . . . . .	146
		5.2.2 Antenna Patterns . . . . .	147
		5.2.3 Beamshape Loss for Different Patterns . . . . .	148
	5.3	Sparse Sampling in 1-D Scan . . . . .	149
		5.3.1 Method of Calculation for 1-D Scan . . . . .	149
		5.3.2 Steady Target Beamshape Loss for 1-D Scan . . . . .	151
	5.3.3	Case 1 Beamshape Loss for 1-D Scan . . . . .	153

5.3.4	Case 2 Beamshape Loss for 1-D Scan . . . . .	155
5.3.5	Beamshape Loss Used in Search Radar Equation for 1-D Scan . . . . .	158
5.4	Sparse Sampling in 2-D Raster Scan . . . . .	160
5.4.1	Method of Calculation for 2-D Scan . . . . .	162
5.4.2	Steady Target Beamshape Loss for 2-D Scan . . . . .	162
5.4.3	Case 1 Beamshape Loss for 2-D Scan . . . . .	163
5.4.4	Case 2 Beamshape Loss for 2-D Scan . . . . .	165
5.4.5	Diversity Target Beamshape Loss for 2-D Scan . . . . .	168
5.4.6	Beamshape Loss in the Search Radar Equation for 2-D Raster Scan . . . . .	171
5.5	Sparse Sampling Using a Triangular Grid . . . . .	174
5.5.1	Method of Calculation for Triangular Grid . . . . .	174
5.5.2	Steady Target Beamshape Loss for Triangular Grid . . . . .	175
5.5.3	Case 1 Beamshape Loss for Triangular Grid . . . . .	175
5.5.4	Case 2 Beamshape Loss for Triangular Grid . . . . .	176
5.5.5	Diversity Target Beamshape Loss for Triangular Grid . . . . .	178
5.5.6	Beamshape Loss in Search Radar Equation for Triangular Grid . . . . .	180
5.6	Summary of Beamshape Loss . . . . .	181
5.6.1	Beamshape Loss for Dense Sampling . . . . .	181
5.6.2	Beamshape Loss for Sparse Sampling . . . . .	182
5.6.3	Processing Methods . . . . .	184
5.6.4	Net Beamshape Loss for the Search Radar Equation . . . . .	185
5.6.5	Beamshape Loss for Unequally Spaced 2-D Scan . . . . .	186
	References . . . . .	186
	Appendix 5A Analytical Approximations for Beamshape Loss . . . . .	188
	5A.1 1-D Beamshape Loss . . . . .	188
	5A.2 2-D Beamshape Loss with Rectangular Grid . . . . .	189
	5A.3 2-D Beamshape Loss with Triangular Grid . . . . .	192
Chapter 6	System Noise Temperature . . . . .	197
6.1	Noise in the Radar Bands . . . . .	197
	6.1.1 Noise Spectral Density . . . . .	197
	6.1.2 Noise Statistics . . . . .	198
6.2	Sources of Noise in Radar Reception . . . . .	200

6.3	Antenna Noise Temperature . . . . .	201
6.3.1	Sources of Antenna Noise Temperature . . . . .	201
6.3.2	Sky Noise Temperature . . . . .	204
6.3.3	Noise Temperature from the Surface . . . . .	209
6.3.4	Noise Temperature from Antenna Ohmic Loss . . . . .	211
6.3.5	Noise Temperature from Antenna Mismatch . . . . .	212
6.3.6	Approximation for Antenna Noise Temperature . . . . .	215
6.4	Receiving Line Temperature . . . . .	217
6.5	Receiver Noise Temperature . . . . .	217
6.5.1	Noise in Cascaded Receiver Stages . . . . .	217
6.5.2	Input and Output Levels . . . . .	219
6.5.3	Quantizing Noise . . . . .	220
6.6	Summary of Receiving System Noise . . . . .	221
6.6.1	Thermal Noise Dependence on Carrier Frequency . . . . .	221
6.6.2	Applicability of Blake's Method . . . . .	222
6.6.3	Refined Method for Modern Radar . . . . .	222
6.6.4	Receiver and Quantization Noise Temperature . . . . .	223
	References . . . . .	223
Chapter 7	Atmospheric Effects . . . . .	225
7.1	Tropospheric Refraction . . . . .	225
7.1.1	Refractive Index of Air . . . . .	226
7.1.2	Standard Atmosphere . . . . .	227
7.1.3	Inclusion of Water Vapor . . . . .	228
7.1.4	Vertical Profile of Refractivity . . . . .	229
7.1.5	Ray Paths in the Troposphere . . . . .	231
7.2	Attenuation in the Troposphere . . . . .	232
7.2.1	Sea-Level Attenuation Coefficients of Atmospheric Gases . . . . .	233
7.2.2	Variation of Attenuation Coefficients with Altitude . . . . .	237
7.2.3	Attenuation Through the Troposphere . . . . .	237
7.2.4	Attenuation to Range $R$ . . . . .	238
7.2.5	Attenuation for Dry and Moist Atmospheres . . . . .	244
7.3	Attenuation from Precipitation . . . . .	246
7.3.1	Rain Attenuation Coefficient at 293K . . . . .	246
7.3.2	Temperature Dependence of Rain Attenuation . . . . .	247
7.3.3	Rainfall Rate Statistics . . . . .	249
7.3.4	Attenuation in Snow . . . . .	251
7.3.5	Attenuation in Clouds . . . . .	253
7.3.6	Weather Effects on System Noise Temperature . . . . .	255
7.4	Tropospheric Lens Loss . . . . .	255

7.5	Ionospheric Effects . . . . .	257
7.5.1	Geometry of Ray in Ionosphere . . . . .	258
7.5.2	Ionospheric Structure . . . . .	258
7.5.3	Total Electron Count . . . . .	260
7.5.4	Faraday Rotation . . . . .	260
7.5.5	Dispersion Across Signal Spectrum . . . . .	264
7.6	Summary of Atmospheric Effects . . . . .	269
	References . . . . .	270
Chapter 8	The Pattern-Propagation Factor . . . . .	273
8.1	Equations for the $F$ -Factor . . . . .	274
8.1.1	Derivation of the $F$ -Factor . . . . .	274
8.1.2	Application of the $F$ -Factor . . . . .	276
8.2	Geometrical Models of the Ray Paths . . . . .	277
8.2.1	Method 1: Flat-Earth Approximation for Distant Target . . . . .	278
8.2.2	Method 2: Flat Earth Approximation with Target at Arbitrary Range . . . . .	279
8.2.3	Method 3: First-Order Approximation for Spherical Earth . . . . .	280
8.2.4	Method 4: Approximation for Spherical Earth with Distant Target $R$ . . . . .	282
8.2.5	Method 5: Approximation for Spherical Earth with Target at Arbitrary Range . . . . .	283
8.2.6	Method 6: Exact Expressions for Spherical Earth with Target at Arbitrary Range . . . . .	285
8.2.7	Comparison of Approximate Methods . . . . .	286
8.3	Reflection Coefficient . . . . .	287
8.3.1	Fresnel Reflection Coefficient . . . . .	288
8.3.2	Reflection from Rough Surfaces . . . . .	292
8.3.3	Land Surfaces with Vegetation . . . . .	295
8.3.4	The Divergence Factor . . . . .	295
8.4	Diffraction . . . . .	296
8.4.1	Smooth-Sphere Diffraction . . . . .	296
8.4.2	Knife-Edge Diffraction . . . . .	299
8.5	The Interference Region . . . . .	302
8.6	The Intermediate Region . . . . .	303
8.6.1	$F$ -Factor as a Function of Range . . . . .	303
8.6.2	$F$ -Factor as a Function of Altitude . . . . .	305
8.6.3	Vertical-Plane Coverage Charts . . . . .	306
8.7	Summary of Propagation Factors . . . . .	309
	References . . . . .	310

Chapter 9	Clutter and Signal Processing . . . . .	311
9.1	Modes of Surface Clutter . . . . .	311
9.1.1	Clutter Cross Section and Reflectivity . . . . .	311
9.1.2	Surface Clutter Pattern-Propagation Factor . . . . .	313
9.1.3	Spectral Properties of Surface Clutter . . . . .	318
9.1.4	Amplitude Distributions of Surface Clutter . . . . .	321
9.2	Models of Sea Clutter . . . . .	323
9.2.1	Physical Properties of the Sea Surface . . . . .	323
9.2.2	Reflectivity of Sea Clutter . . . . .	324
9.2.3	Power Spectrum of Sea Clutter . . . . .	326
9.2.4	Amplitude Distribution of Sea Clutter . . . . .	327
9.3	Models of Land Clutter . . . . .	327
9.3.1	Reflectivity of Land Clutter . . . . .	329
9.3.2	Power Spectrum of Land Clutter . . . . .	331
9.3.3	Amplitude Distribution of Land Clutter . . . . .	332
9.4	Discrete Clutter . . . . .	333
9.4.1	Discrete Land Features . . . . .	333
9.4.2	Birds and Insects . . . . .	333
9.4.3	Land Vehicles . . . . .	334
9.4.4	Wind Turbines . . . . .	335
9.5	Models of Volume Clutter . . . . .	335
9.5.1	Volume Clutter Cross Section and Reflectivity . . . . .	336
9.5.2	Volume Clutter Pattern-Propagation Factor . . . . .	337
9.5.3	Spectral Properties of Volume Clutter . . . . .	338
9.5.4	Amplitude Distribution of Volume Clutter . . . . .	340
9.5.5	Precipitation Clutter Models . . . . .	340
9.5.6	Chaff Models . . . . .	343
9.6	Clutter Improvement Factor . . . . .	344
9.6.1	Coherent MTI Improvement Factors . . . . .	345
9.6.2	Noncoherent MTI Improvement Factors . . . . .	347
9.6.3	Other MTI Considerations . . . . .	347
9.6.4	Pulsed Doppler Processing . . . . .	348
9.6.5	Clutter Maps . . . . .	352
9.7	Summary of Clutter and Signal Processing . . . . .	352
	References . . . . .	353
Chapter 10	Loss Factors in the Radar Equation . . . . .	357
10.1	Reduction in Received Signal Energy . . . . .	358
10.1.1	Terms Specified in the Radar Equation . . . . .	358
10.1.2	Components of Range-Dependent Response Factor $F_{\text{rdr}}$ . . . . .	361
10.1.3	Losses Included in System Noise Temperature . . . . .	364

10.1.4	Losses in Search Radar Equation . . . . .	364
10.1.5	Losses Included in Antenna Gain . . . . .	367
10.2	Increases in Required Signal Energy . . . . .	370
10.2.1	Statistical Losses . . . . .	370
10.2.2	Losses in Basic Detectability Factor . . . . .	374
10.2.3	Matching and Bandwidth Losses . . . . .	375
10.2.4	Beamshape Loss $L_p$ . . . . .	378
10.2.5	Signal Processing Losses . . . . .	379
10.2.6	Losses in Clutter Detectability Factor . . . . .	388
10.3	Losses in Visual Detection . . . . .	394
10.3.1	Losses in the Visibility Factor . . . . .	394
10.3.2	Collapsing Loss on the Display . . . . .	394
10.3.3	Bandwidth Correction Factor $C_b$ . . . . .	395
10.3.4	Operator Loss $L_o$ . . . . .	395
10.4	Summary of Loss Factors . . . . .	396
	References . . . . .	397
	List of Symbols . . . . .	399
	Appendix Analysis Tools on DVD . . . . .	411
	About the Author . . . . .	419
	Index . . . . .	421



# Preface

The starting point for analysis of radar performance is the *radar range equation*, which gives the maximum range at which a specified signal-to-noise ratio, required for successful detection of a target, can be obtained. The physical principles behind what is usually called simply the *radar equation* have been known since the work performed during World War II and reported in the unclassified post-war paper by Norton and Omberg.<sup>1</sup> Subsequent books on radar systems, starting with Ridenour's *Radar System Engineering* in 1947, have included chapters in which the equation is derived and expressed in different ways, with terms characterizing the radar, the target, the detection requirements, and the environment in which the radar operates. The complexity of environmental effects leads most of these discussions to presentation of an equation giving the range in an environment where thermal noise is the only source of interference competing with the target echo, and where the path between the radar and the target is characterized by a range-dependent atmospheric attenuation factor.

The most thorough discussion of the radar equation appeared in Blake's *Radar Range-Performance Analysis*, based on work by that author at the Naval Research Laboratory between 1940 and 1972, and published in 1980. That book is of lasting value and remains in print after more than thirty years. The reader is urged to obtain and read it.

The objective of this new volume is to extend Blake's classic work to ensure applicability of radar equations to design and analysis of modern radars, to identi-

---

<sup>1</sup> See the list of references at the end of Chapter 1.

fy what information on the radar and its environment is needed to predict detection range, and to provide equations and data to improve the accuracy of range calculations. The chapter outline follows generally that of Blake's book so that the reader can better appreciate his contributions while identifying extensions that are useful in application to modern radars. Special attention is directed to propagation effects, methods of range calculation in environments that include clutter and jamming in addition to thermal noise, and to establishing the many loss factors that reduce radar performance.

There are two conflicting approaches to deriving a radar equation. Following the Naval Research Laboratory work of World War II and Blake's elegant extensions, we adopt here the first approach. In addition to the standard geometrical relationships for a wave spreading as it moves through space, it uses the concept of the *matched filter*, in which the ratio of input signal energy to noise spectral density, during the *observation time* on the target, is used to calculate the *maximum possible* output signal-to-noise (power) ratio SNR that would be obtained in an ideal (lossless) system. The input signal *energy* is proportional to the average power of the transmission, regardless of its waveform. A succession of loss factors is applied to find the output SNR for the practical radar being considered, as a function of the target range. The detection range is then the range at which that SNR meets the requirement for a stated probability of detection, given a required false-alarm probability. That requirement is identified as the *detectability factor*, and it depends on details of the practical signal processing method used in the radar.

Following the first approach, the efficiency of the radar can be compared to that of an "ideal" system in terms of the total of losses that have been introduced the practical implementation. Inspection of the loss budget may suggest improvements in design or modeling, but performance beyond that of the ideal system is clearly ruled out.

The alternative approach calculates the output SNR of a single pulse at the receiver output as a *power ratio*, dependent on such parameters as receiver bandwidth, peak power of the transmission, and many other factors in design of the practical radar. In most cases that SNR is inadequate for reliable detection, and a succession of *processing gains* is applied to bring it to the required level at some calculated detection range. That evaluation, if correctly performed, would give the same range as the first approach.

The hazard in the second approach is that no theoretical limit to performance is established as a check on how much processing gain is theoretically available. The receiver bandwidth and processing gains in a modern radar, using complex pulse-compression waveforms, mixtures of coherent and noncoherent integration, and digital processing, are difficult to define. Too many cases have occurred in which the calculated performance exceeds that available from a matched-filter system, as cascaded gains are applied incorrectly to the analysis.

Blake's work was motivated by the requirement that Naval Research Laboratory perform accurate evaluations of competing contractor proposals for new naval radar designs. It provided a means of comparing systems when detailed information was omitted or described in a way that protected "proprietary technology." The *Blake Chart*, discussed here in Chapter 1, became the gold standard for clarifying issues of radar range performance. Open publications of the work allowed radar professionals to obtain reproducible results on a wide variety of radar system designs.

What is surprising is that subsequently published radar texts fail to take advantage of this work. Blake contributed the chapter on the radar equation to the 1970 and 1990 editions of Skolnik's *Radar Handbook*, but to this day other texts continue to use radar equations in which a "receiver bandwidth  $B$ " appears in the denominator of the equation to give receiver "noise power" that is proportional to that bandwidth. The radar novice might conclude that as  $B \rightarrow 0$  the  $\text{SNR} \rightarrow \infty$ , although disabling the receiver does not improve its detection performance. Transmission of a pulse-compression waveform having  $B = 100$  MHz yields a noise bandwidth  $B_n = 100$  MHz for the matched pulse-compression filter, according to the accepted definition of that term given in Chapter 6 of this book. A large "pulse-compression gain" must be included somewhere in the equation if that bandwidth is used in the denominator. Similar confusion applies when digital Doppler filtering is used with a coherent pulse train, or when multiple pulses are integrated after envelope detection.

Experience shows that a radar range equation containing receiver bandwidth  $B$  has a high probability of causing serious errors, which can be avoided using Blake's approach.

Another source of error is using noise figure  $F$  and a standard temperature  $T_0 = 290\text{K}$  in the denominator of the radar equation. When the product  $N = kT_0FB$  is used for noise power, the result is pessimistic for radars that look into a cold sky. An alternative form appearing in at least one recent text substitutes the expression  $N = kT_0(F - 1)B$ , which predicts that  $N \rightarrow 0$  as  $F \rightarrow 1$ . This leads to optimistic results for any radar operating in an environment with temperature above  $-273^\circ$  Celsius. Blake addresses this problem in a way that achieves accurate results for any environment, as discussed here in Chapter 6.

Blake's inclusion of the pattern-propagation factors  $F_t$  and  $F_r$  in the radar equation addresses a host of problems that complicate range calculation. Omission of that factor from presentation of the equation, even when propagation effects are discussed elsewhere in a text, invites error.

Given that Blake uses the approach in his papers and textbook that avoids these errors, what justifies a new book on the subject?

First, equations for detection in environments in which clutter and jamming add to thermal noise are discussed only briefly by Blake. More detailed treatment is needed, especially in the case of clutter, which cannot be modeled by a Gaussi-

an probability density function and a uniform spectral density. This subject is covered here in Chapters 3 and 9.

Second, use of diversity (in time, frequency, space, or polarization) is an important method of minimizing the energy required for detection probabilities greater than 50%. This subject is explored in detail in Chapter 4. That chapter presents methods not discussed by Blake or the collaborator in his text by which the detectability factor can be calculated on personal computers for different radar and target models that provide measures of diversity to reduce the detectability factor.

Third, new radar technology such as active phased arrays presents problems in analysis that were not anticipated in Blake's work. For example, the multifunction array radar (MFAR) must often economize on scan time by minimizing overlap in beam positions. The optimization of beam spacing during scanning of a volume requires a compromise between scan time and total energy expended to achieve the required detection probability. This subject is explored in Chapter 5.

Fourth, much of Blake's material involves a mixture of metric and "U.S. customary units" such as nautical miles and kilofeet. We have found that consistent use of metric units in radar performance analysis avoids introducing errors in conversions to and from other systems. When presenting results to U.S. Navy or Air Force personnel or others unaccustomed to using metric units, a simple conversion after completion of the analysis provides the modified data with minimal opportunity for error.

Lastly, this writer hopes that Blake's legacy to the profession will not be compromised by calling attention to an inconsistency in use of his *bandwidth correction factor*  $C_b$  as a factor multiplying the detectability factor in the denominator of the radar equation (see Section 1.3). That factor, as defined and plotted by Blake, is unity for an optimum product of bandwidth and pulsewidth  $B_r\tau \approx 1.2$ , and hence is applicable only to multiply the *visibility factor* of a cathode-ray-tube display. If it is applied to multiply the detectability factor for electronic detection, the result is optimistic by  $\approx 2$  dB, an error which is inconsistent with the accuracy desired and available from the rest of Blake's approach.

What accuracy should be expected of range calculations using the radar equation? Blake discusses this issue at the end of his chapter on pulse-radar detection-range computation without arriving at numerical estimates. Marcum, in his classic work on detection theory,<sup>2</sup> warned of pitfalls in range calculation:

The number of pitfalls that may be encountered in the use of the [radar] equation are almost without limit, and many of these difficulties have been recognized in the past

He goes on to mention three of the most troublesome as evaluation of the target cross section, the minimum discernible signal power, and the statistical nature of detection range as a function of detection probability. To his list we must add

---

<sup>2</sup> See reference [4] of Chapter 4.

the uncertainty in target location relative to points of maximum radar system response in four-dimensional radar space, and the presence of other than thermal noise in the environment.

Even in cases where only thermal noise is present, the accuracy can seldom be better than about three decibels in required and achieved energy ratio (equivalent to about 20% in free-space range). In a clutter environment, reduced accuracy is inevitable, and the resulting error in range, even for 3-dB error in signal-to-clutter ratio, may exceed 20%.

It remains useful to perform calculations to precisions of a fraction of one decibel. This permits alternative designs to be compared with greater precision, and loss budgets to be evaluated as a guide to improved designs. With careful modeling, it is unnecessary to add several decibels of error to that caused by uncertainties in the environment or the performance of radar operating and maintenance personnel. When radar performance in field tests fails to measure up to specifications and predictions, it is common to attribute the difference to a “field service loss” or “operator loss” of several decibels, when in fact the performance was never designed into the radar system.

This book is intended to provide methods by which the errors in predicting radar range performance can be minimized, even though they cannot be avoided completely.

The author would like to express his thanks to Dr. Paul Hamilton for his review of the manuscript during its generation, and to many colleagues, especially Harold Ward and William Shrader, whose advice over many years has been essential to understanding the factors that affect radar detection range. Lamont Blake was one of those colleagues, and his insights will continue to guide the future efforts of the radar community.

# CHAPTER 1

## Development of the Radar Equation

The radar range equation was developed during World War II to permit analysis of radar system performance and to guide radar developers in choosing among the limited design options available in that era. The earliest literature on the subject was subject to military security restrictions but was published after the end of the war and has been widely distributed.

The basic approach to predicting radar detection range has remained consistent with the early work, summarized in the first published paper on the radar equation: the 1947 paper by Norton and Omberg of the U.S. Naval Research Laboratory [1, 2]. We will refer to that equation as the *original radar equation*. In this chapter we review the steps by which the radar equation was developed, and discuss its evolution to forms that can be applied to analysis and design of modern radar systems. To avoid confusion from varied symbols used by different authors, we replace those used in the referenced works with a consistent system of symbols, defined as they occur and listed in Appendix A at the end of this book. This permits direct comparison of the equations and their limitations and applicability to current problems.

### 1.1 RADAR EQUATION FUNDAMENTALS

The objective of the radar equation is to calculate the maximum range  $R_m$  at which the desired detection performance can be achieved for a specified set of radar, target, and environmental parameters. The radar equation discussed in this chapter is limited to an environment in which thermal noise is the only source of interference against which a target echo signal must successfully compete to be detected. Equations for other environments are developed in Chapter 3.

The radar range equation is derived in three steps:

1. Express the *maximum* signal-to-noise ratio that is *available* with given parameters, as a function of range;
2. Express the *minimum* signal-to-noise ratio that is *required* to meet detection requirements;
3. Combine these expressions to solve for the *maximum* range at which the requirement is met for the specified radar.

### 1.1.1 Maximum Available Signal-to-Noise Ratio

It was determined in classified work by North during World War II [3], subsequently reprinted in *Proceedings of the IEEE*, that the maximum possible signal-to-noise power ratio  $(S/N)_{\max}$  is obtained when the receiving system uses the *matched filter* for the transmitted waveform. This maximum ratio is equal to the energy ratio  $E/N_0$  of the waveform,<sup>1</sup> where  $E$  is the energy of the echo signal and  $N_0$  is the spectral density of competing thermal noise. The expression to be developed in step 1 gives  $E/N_0$  for the specified system parameters. In [1],  $E/N_0$  is defined as the available energy ratio of a single pulse, referred to the output port of the receiving antenna. That reference point is used throughout this book.

The energy density  $E_p$  of the outgoing pulse, measured at an arbitrary range  $R$  from an isotropic transmitting antenna, is

$$E_p = \frac{E_t}{4\pi R^2} \quad (\text{J/m}^2) \quad (1.1)$$

where  $E_t$  (joules) is the energy of the transmitted pulse and  $4\pi R^2$  is the area of a sphere of radius  $R$  centered on the radar. For an assumed rectangular pulse of width  $\tau$  (s) and peak power  $P_t$  (W),  $E_t = P_t\tau$  (J). For a transmitting antenna with gain  $G_t$ , the energy density on the axis of the beam is increased by that gain:

$$E_p = \frac{E_t G_t}{4\pi R^2} = \frac{P_t \tau G_t}{4\pi R^2} \quad (\text{J/m}^2) \quad (1.2)$$

After reflection from a target having a radar cross section  $\sigma$  ( $\text{m}^2$ ), the energy density  $E_a$  of the echo incident on the radar receiving antenna is

$$E_a = \frac{E_p \sigma}{4\pi R^2} = \frac{P_t \tau \sigma}{(4\pi R^2)^2} \quad (\text{J/m}^2) \quad (1.3)$$

Equation (1.3) follows from the definition of radar cross section [4].

---

<sup>1</sup> Note that *energy ratio* in this book is  $E/N_0$ , not  $\mathcal{R} = 2E/N_0$  used in some texts.

The radar receiving antenna with effective aperture  $A_r$  captures energy  $E$  given by

$$E = E_a A_r = \frac{P_t \tau G_t A_r \sigma}{(4\pi R^2)^2} \quad (\text{J}) \quad (1.4)$$

Using the expression for receiving antenna gain

$$G_r = \frac{4\pi A_r}{\lambda^2} \quad (1.5)$$

where  $\lambda$  is wavelength, we obtain the desired equation for the maximum available signal energy at the output port of a pulsed radar receiving antenna:

$$E = \frac{P_t \tau G_t G_r \lambda^2 \sigma}{(4\pi)^3 R^4} \quad (\text{J}) \quad (1.6)$$

So far we have considered an ideal case in which the transmitter delivers its output directly to the antenna, and where there are no losses along the transmitter-target-receiver path that reduce the received signal energy. To allow for such radio-frequency (RF) losses, a factor  $L_1$  can be included in the denominator, yielding

$$E = \frac{P_t \tau G_t G_r \lambda^2 \sigma}{(4\pi)^3 R^4 L_1} \quad (\text{J}) \quad (1.7)$$

The derivation of (1.7) follows the procedure presented in today's radar texts, but differs from many of these in expressing the *energy* of the transmitted and received pulses rather than *power*.

To find the available energy ratio, the noise spectral density  $N_0$  (W/Hz), referred to a receiver connected directly to the antenna output port, is expressed as

$$N_0 = kT_s \quad (\text{W/Hz or J}) \quad (1.8)$$

where

$k = 1.38 \times 10^{-23}$  J/K is Boltzmann's constant;

$T_s =$  system noise temperature in kelvins (K) (see Chapter 6).

Combining (1.7) and (1.8), we obtain the maximum available signal-to-noise power ratio:

$$\left(\frac{S}{N}\right)_{\max} = \frac{E}{N_0} = \frac{P_r \tau G_t G_r \lambda^2 \sigma}{(4\pi)^3 R^4 k T_s L_1} \quad (1.9)$$

### 1.1.2 Minimum Required Signal-to-Noise Ratio

The second expression used in derivation of the radar equation gives the energy ratio required to obtain the specified detection performance. It is assumed in [1] that detection is performed by a human operator observing a cathode-ray-tube display that presents  $n$  successive echo pulses:

$$V(n) = \frac{E_{\min}}{N_0} \quad (1.10)$$

where  $E_{\min}$  is the minimum energy of each received pulse that renders the  $n$ -pulse group visible on the display under optimum viewing conditions. This is consistent with the current definition [4]:

**visibility factor (pulsed radar)** The ratio of single-pulse signal energy to noise power per unit bandwidth that provides stated probabilities of detection and false alarm on a display, measured in the intermediate-frequency portion of the receiver under conditions of optimum bandwidth and viewing environment.

The minimum required energy is thus

$$E_{\min} = N_0 V(n) = k T_s V(n) \quad (\text{J}) \quad (1.11)$$

The number of pulses  $n$  is given by the product of the pulse repetition frequency  $f_r$  and the observation time  $t_o$ , which is the lesser of the dwell time of the radar beam on the target or the time constant of the display and human observer:

$$n = f_r t_o \quad (1.12)$$

Thus the required energy ratio can be reduced by integration of successive pulses obtained with broad beams or slow scanning of the radar across the target position.

Experimental values for  $V(n)$  with an optimum A-scope<sup>2</sup> were reported in [5]. These and similar results for the PPI displays<sup>3</sup> are presented in [6–12]. For radar systems in which electronic detection replaces visual detection, the visibility factor is replaced by a *detectability factor*  $D(n)$ , defined [4]:

<sup>2</sup> The A-scope displays receiver output voltage vs. range.

<sup>3</sup> The PPI displays receiver voltage as intensity on a polar plot of range vs. azimuth angle.

In pulsed radar, the ratio of single-pulse signal energy to noise power per unit bandwidth that provides stated probability of detection for a given false alarm, probability, measured in the intermediate-frequency amplifier bandwidth and using an intermediate-frequency filter matched to the single pulse and followed by optimum video integration.

Subscripts are sometimes added to  $V$  and  $D$  to denote the target model and the detection probability to which they apply (e.g.,  $V_{0(50)}$ , denoting the energy ratio required for 50% probability of detection on a steady (Case 0) target [6–12]). In general,  $V$  exceeds  $D$  as a result of the lower efficiency of the visual detection process, as discussed in Section 4.6.

### 1.1.3 Maximum Detection Range for Pulsed Radar

Setting the available  $E/N_0$  in (1.9) equal to the required value  $V$  or  $D$ , the equation for maximum range of a pulsed radar is obtained:

$$\text{For visual detection: } R_m = \left[ \frac{P_t \tau G_t G_r \lambda^2 \sigma}{(4\pi)^3 k T_s V(n) L_1} \right]^{1/4} \quad (\text{m}) \quad (1.13)$$

$$\text{For electronic detection: } R_m = \left[ \frac{P_t \tau G_t G_r \lambda^2 \sigma}{(4\pi)^3 k T_s D(n) L_1} \right]^{1/4} \quad (\text{m}) \quad (1.14)$$

These equations are only the starting point for prediction of radar detection range. They give the range along the axis of a common transmitting-receiving antenna beam at which the received energy ratio is adequate under free-space conditions, when using an optimum filter (for visual detection) or a matched filter (for electronic detection).

## 1.2 The Original Radar Equation

The range equation derived by Norton and Omberg [1] is expressed by (1.13), with the following understandings:

- *Noise Spectral Density.* The noise power spectral density calculated as

$$N_0 = kTF_n \quad (\text{W/Hz}) \quad (1.15)$$

for a system at a “room temperature”  $T = 300\text{K}$  with receiver noise figure  $F_n$ .

- *Visibility Factor.* The visibility factor is derived for a pulse “barely visible” on an A-scope display [5], and is defined to include the effects of

nonoptimum bandwidth rather than using separate values of an ideal visibility factor, as defined in [4], and a bandwidth correction factor, introduced in [6–12].

- *Propagation Effects.* The authors in [1] discuss the effects of tropospheric absorption and refraction and reflections from the surface underlying the radar-target path, but these are not included as terms in the original radar equation.
- *RF Losses.* Transmitting and receiving line losses  $L_t$  and  $L_r$  are included in a final equation in [1] based on (1.13). That form of the equation, complicated by several numerical conversion constants, is no longer useful.

A numerical conversion factor is introduced in [1] to present the resulting range in miles. Other numerical factors are introduced by substitution for the constants  $4\pi$ ,  $k$ , and  $T$ , and by inclusion of approximations for visibility factor and target cross section, such that the final expression is encumbered by a numerical constant that obscures the basic relationships used in derivation. This was done to combine as many factors as possible into a single numerical value in an era when calculations were made by slide rule or electromechanical calculators. That is no longer necessary or desirable. In order to expose the relationships and permit comparison of different forms of the radar equation, we retain in subsequent discussion the terms used in derivation, without conversion factors or introduction of numerical values.

In spite of these limitations, the original radar equation, formulated during World War II, remains relevant today in that it uses the signal-to-noise energy ratio to capture the fundamental relationships between detection range for a free-space path and parameters of the radar and target. The insight of the originators of this equation, in relying on North's matched-filter relationship and using energy ratios as the criterion for successful detection, deserves the recognition accorded by Blake and overlooked in much of the current literature.

### 1.3 BLAKE'S RADAR EQUATION FOR PULSED RADAR

Lamont V. Blake at the Naval Research Laboratory [6–13] builds on the World War II work, while introducing more precise definitions of terms in the radar equation. His basic radar range equation for pulsed radar takes the form [12, p. 19, Eq. (1.34)]:

$$R_m = \left[ \frac{P_t \tau G_t G_r \lambda^2 \sigma F_t^2 F_r^2}{(4\pi)^3 k T_s D(n) C_b L} \right]^{1/4} \quad (\text{m}) \quad (1.16)$$

The numerator of (1.16) has dimension  $\text{J}\cdot\text{m}^4$ , when the terms are expressed in fundamental units. The new terms added to (1.14) are:

- $F_t$  = pattern-propagation factor for the transmitting path;  
 $F_r$  = pattern-propagation factor for the receiving path (see Chapter 8).

The denominator of (1.16) has dimension J, where the new terms are:

- $T_s$  = system input temperature in kelvins (see Chapter 6);  
 $D(n)$  = detectability factor (defined in Section 1.1.2; see Chapter 4);  
 $C_b$  = bandwidth correction factor (see Section 10.2.3);  
 $L$  =  $L_1 L_2$  = system loss factor.

The system loss  $L$  is expressed by the product of two components:  $L_1$ , the RF loss in (1.7) that reduces the available energy ratio, and  $L_2$ , the signal processing loss that increases the required energy ratio relative to  $D(n)$ .

### 1.3.1 Significance of Terms in Blake's Equation

The terms in Blake's radar equation are defined to provide accurate results for pulsed radars with or without intrapulse modulation, using noncoherent integration, and operating in the natural environment. Attention should be paid to following factors.

- *Transmitter Energy.* The use of pulse energy  $P_t \tau$  allows (1.16) to be applied directly to radars using pulse compression waveforms for which the time-bandwidth product  $\tau B \gg 1$ , where  $B$  is the width of the transmitted pulse spectrum. This contrasts with equations in which  $P_t$  is used without  $\tau$  in the numerator, and a competing noise power  $N_0 B$  appears in the denominator. Such equations are inapplicable to transmissions with intrapulse modulation.
- *Pattern-Propagation Factors.* Blake introduces directly into the radar equation the factors  $F_t$  and  $F_r$  that account for the elevation pattern of the antenna and the effects of surface reflections, both functions of elevation angle and essentially invariant with range. The pattern-propagation factor is defined [14, p. 35] as

the ratio of the amplitude of the electric field at a given point under specified conditions to the amplitude of the electric field under free-space conditions with the beam of the transmitter directed toward the point in question.

- As used in (1.16), this factor is understood to exclude the effects of the azimuth antenna pattern and attenuation of the medium, both of which Blake includes as components of  $L$ . The  $F$  factors include the antenna gains at the target elevation relative to those on the axes at which  $G_t$  and  $G_r$  are defined, the contribution of surface reflections to the radiated and received fields, and modification of the fields by diffraction on low-elevation paths. For array antennas, they include also the reduced gain from off-broadside operation, calculation of which is discussed in Chapter 10.

- *Noise Temperature.* Blake introduces the system noise temperature  $T_s$  to express the effects of both internal and external noise sources, replacing the product  $TF_n$  in (1.15). This change is especially important when the receiver noise figure is small and the antenna beam points into the cold sky. It should be noted that  $T_s$  is referred to the output terminal of the receiving antenna, and includes the effects of thermal noise output from the antenna and receiving line loss  $L_r$  between the antenna and the receiver, as well as that from the receiver itself.
- *Use of Energy Ratios.* Blake continues the use of energy ratios for the available and required signals, as in the original radar equation.
- *Detectability Factor.* The detection process can be either electronic or visual, but any departure from the ideal process that is assumed in deriving the detectability factor requires inclusion of an appropriate component in the loss factor  $L_2$ .
- *Bandwidth Factor.* The factor  $C_b$ , is given by [12, Eq. (8.14a)] as

$$C_b = \frac{B_n \tau}{4.8} \left( 1 + \frac{1.2}{B_n \tau} \right)^2 \quad (1.17)$$

where  $B_n$  is the noise bandwidth of the receiver. This factor is equal to unity for an “optimum” receiver noise bandwidth  $B_n = 1.2/\tau$ . Its origin and use are discussed in Section 10.3.3, and the error arising from use of  $C_b$  in radars with electronic detection is discussed in Section 1.5.4.

- *Loss Factor.* The system loss factor  $L$ , appearing in (1.16), is the product of the following factors:

$L_t$ , transmission line loss in the path connecting the transmitter output to the antenna terminal at which  $G_t$  is measured;

$L_\alpha$ , atmospheric absorption loss for the two-way path;

$L_p$ , beamshape loss<sup>4</sup> for a scanning radar [13];

$L_x$ , miscellaneous signal processing loss that represents the product of other receiving and signal processing losses not specifically included in  $T_s$ ,  $C_b$ ,  $L_p$ , or  $L_\alpha$ .

Of these losses,  $L_t$  and  $L_\alpha$  contribute to the RF loss  $L_1$  that decreases available on-axis energy ratio, while  $L_p$  and  $L_x$  contribute to the loss  $L_2$  that increases required energy ratio. The treatment of loss factors and the fact that some are functions of the required detection probability are discussed in detail in Chapters 4 and 10.

---

<sup>4</sup> Blake refers to this as “antenna pattern loss,” but beamshape loss is the original and currently accepted term. This loss is discussed in detail in Chapter 5.

### 1.3.2 Methods of Solving for Range

Because of the complicated range-dependence of the terms  $F_t$ ,  $F_r$ , and  $L_{\alpha}$ , there is no closed-form solution for  $R_m$  using (1.16). Blake discusses iterative and graphical methods for solution [12, pp. 379–388]. One simple method is embedded in the “Pulse-Radar Range-Calculation Worksheet,” commonly known as the *Blake chart*, shown in Figure 1.1. This chart is used to solve the equation by addition and subtraction of decibel values, easily performed with pocket calculators.

The antenna height above the surrounding surface and the target elevation angle are entered in the Blake chart for record, because the result is only valid for those specific conditions. The user then enters five parameters in part (1), using them to calculate the system noise temperature  $T_s$ . The terms listed as coming from figures and tables are discussed in Chapter 6, where the applicable figures are presented along with equations to replace conversion tables. Remaining range factors are entered in part (2) of the chart, converted to decibel form in part (3), and summed to find the decibel value  $40 \log R_{0(\text{nmi})}$ . The free-space range  $R_0$  in nautical miles is found as the antilogarithm. The pattern-propagation factor  $F$  is calculated separately (see Chapter 8), and multiplies  $R_0$  to obtain an initial range estimate  $R'$ . That estimate is input to a two-stage iteration to correct for atmospheric attenuation. Additional iteration steps may be required when the attenuation coefficient of the atmosphere at the target is large, as in some millimeter-wave radar cases or in microwave radar when precipitation is present.

A complication in the Blake chart is the use of mixed units for entry of range factors. These include the radar frequency  $f_{\text{MHz}} = (c/\lambda)/10^6$  rather than  $\lambda$  that appears in the radar equation. The resulting range-equation constant collects the several conversion factors, constants, and their dimensions as:

$$\begin{aligned} & 10 \log \left[ \frac{(10^3 \text{ W/kW})(10^{-6} \text{ s}/\mu\text{s})(3 \times 10^8 \text{ m/s})^2}{(4\pi)^3 (1.38 \times 10^{-23} \text{ W} \cdot \text{s/K})(185,200 \text{ m}/100 \text{ nmi})^4} \right] \\ &= 10 \log \left[ 1.292^4 \left( \text{K} \cdot \text{nmi}^4 / \text{W} \cdot \text{s}^3 \cdot \text{m}^2 \right) \right] \\ &= 4.45 \text{ dB} \left[ \text{ref} \left( \text{K} \cdot \text{nmi}^4 / \text{W} \cdot \text{s}^3 \cdot \text{m}^2 \right) \right] \end{aligned}$$

Note that a median radar cross section  $\sigma_{50}$  and a corresponding visibility factor  $V_{0(50)}$  are entered into the Blake chart, to arrive at the range  $R_{50}$  for a probability of detection  $P_d = 50\%$ . The radar cross section normally specified is its average value, which for a fluctuating target characterized as Swerling Case 1 (see Section 4.3.3) is 1.5 dB greater than the median.

PULSE-RADAR RANGE-CALCULATION WORK SHEET

1. Compute system input noise temperature,  $T_{NI}$ , following outline in section (1) below.
2. Enter range factors known in other than decibel form in section (2) below, for reference.
3. Enter logarithmic and decibel values in section (3) below, positive values in plus column, negative in minus. (Example: If  $V_{o(50)(db)}$  as given by Fig. A1 or A2 is negative, then  $-V_{o(50)(db)}$  is positive, goes in plus column.) To convert range factors to decibel values, use Table A2. For  $C_{B(db)}$  use Fig. A3.

Radar antenna height:  $h =$  ft. Target elevation angle:  $\theta =$  °. (See Fig. A12).

(1) COMPUTATION OF $T_{NI}$ : $T_{NI} = T_a + T_{r(I)} + L_r T_e$	(2) RANGE FACTORS		(3) DECIBEL VALUES		PLUS (+)	MINUS (-)
		$P_t(kw)$		$10 \log P_t(kw)$	-	.
	$\tau_{\mu sec}$		$10 \log \tau_{\mu sec}$		.	.
(a) For general range computation, use Figure A5 for $T_a$ .	$G_t$		$G_t(db)$		.	.
	$G_r$		$G_r(db)$		.	.
(b) To find $L_r$ , given $L_r(db)$ , use first and second columns of Table A2.	$\sigma_{50(sq.m.)}$		$10 \log \sigma_{50}$		.	.
	$f_{Mc}$		$-20 \log f_{Mc}$		.	.
	$T_{NI}$ , °K		$-10 \log T_{NI}$		.	.
(c) Also in Table A2, opposite $L_r(db)$ in first column, read $T_{r(I)}$ in third column.  Note: If thermal temperature ( $T_e$ ) of transmission line is appreciably different from 290°K, multiply Table A2 values of $T_{r(I)}$ by $T_e/290$ .	$V_{o(50)}$		$-V_{o(50)(db)}$		.	.
	$C_B$		$-C_B(db)$			.
	$L_t$		$-L_t(db)$			.
	$L_p$		$-L_p(db)$			.
	$L_x$		$-L_x(db)$			.
	Range-equation constant ( $40 \log 1.292$ )					4.45
(d) Opposite $\overline{NF}_{db}$ in first column, read $T_e$ in third col.	4. Obtain column totals →				.	.
	5. Enter smaller total below larger →				.	.
	6. Subtract to obtain net decibels →				+	.

$T_t$		$T_a$	
$L_r$		$T_{r(I)}$	
$\overline{NF}_{db}$		$L_r T_e$	
$T_e$		$T_{NI}$	

7. In Table A3, find range ratio corresponding to this net decibel value, taking its sign (+) into account. Multiply this ratio by 100. This is  $R_o$  →

8. Multiply  $R_o$  by the pattern-propagation factor.  
 $F =$   See Eqs. 27 - 44, and Figs. 8 - 12.  
 $R_o \times F = R'$  →

9. On the appropriate curve of Figures A6 - A11, determine the atmospheric-absorption loss factor,  $L_{a(db)}$ , corresponding to  $R'$ . This is  $L_{a(db)(1)}$  →

10. In Table A3, find the range-decrease factor corresponding to  $L_{a(db)(1)}$ ,  $\delta_1$  →

11. Multiply  $R'$  by  $\delta_1$ . This is a first approximation of the range,  $R_1$  →

12. If  $R_1$  differs appreciably from  $R'$ , on the appropriate curve of Figures A6 - A11 find the new value of  $L_{a(db)}$  corresponding to  $R_1$ . This is  $L_{a(db)(2)}$  →

13. In Table A3, find the range-increase factor corresponding to the difference between  $L_{a(db)(1)}$  and  $L_{a(db)(2)}$ . This is  $\delta_2$ . →

14. Multiply  $R_1$  by  $\delta_2$ . This is the radar range in nautical miles,  $R_{50}$  →

Note: If the difference between  $L_{a(db)(1)}$  and  $L_{a(db)(2)}$  is less than 0.1 db,  $R_1$  may be taken as the final range value, and steps 12 - 14 may be omitted. If  $L_{a(db)(1)}$  is less than 0.1 db,  $R'$  may be taken as the final range value, and steps 9 - 14 may be omitted. (For radar frequencies up to 10,000 megacycles, correction of the atmospheric attenuation beyond the  $L_{a(db)(2)}$  value would amount to less than 0.1 db.)

Figure 1.1 Blake's Pulse-Radar Range-Calculation Worksheet [8]. The referenced figures are reproduced in Chapters 4, 6 and 7, and the referenced tables for conversions between decibels and ratios are now replaced by digital calculation.

Plots of  $V_{0(50)}$  and corresponding  $D_{0(50)}$  for electronic detection are presented in [6–8], but calculations for values of  $P_d$  other than 50% are often needed. Blake's subsequent presentations in [9–12] provide plots of  $D$  for different values of  $P_d$  and for several target models. These plots require use of the average (rather than the median) value of  $\sigma$  in (1.16) and in the Blake chart.

### 1.3.3 Advantages of the Blake Chart

A major advantage of the Blake chart is that it records the input values on which the range calculation is based, along with several intermediate results. In the absence of this discipline, essential data may be left unrecorded and unavailable for later reference. When engineering calculators or digital computer methods are used to replace Blake's conversion tables and manual intermediate steps, the process is rapid and accurate. The exact form of the chart has undergone successive modifications from Blake's original in [6] to its final form in [12], but the basic approach remains. A modification of the chart that maintains entries in fundamental units is described in Section 1.4.2.

The Blake chart formalizes the iteration that solves for the effects of range-dependent attenuation. It has been widely accepted as a standard range-calculation method, although parameters would preferably be entered in fundamental units. Procedures for conversions between decibels and ratios no longer require recourse to associated tables because they are performed readily on pocket calculators or computers. Preservation of the basic format of the chart remains an important element in providing traceability of results. There are all too many opportunities for error when the entire process is reduced to entry of parameters into a computer program and reading an output representing detection range, without recording and inspection of inputs and intermediate results.

### 1.3.4 Blake's Coherent Radar Equation

Blake extends (1.16) to coherent radars [12, p. 20, Eq. (1.35)]:

$$\text{Coherent radar: } R_m = \left[ \frac{P_{av} t_f \tau G_t G_r \lambda^2 \sigma F_t^2 F_r^2}{(4\pi)^3 k T_s D(1) C_b L} \right]^{1/4} \quad (\text{m}) \quad (1.18)$$

Here the energy  $P_{av} t_f$  of the observed waveform replaces the single-pulse transmitted energy  $P_t \tau = P_{av} t_r$ , where  $P_{av}$  is average power,  $t_f$  is the coherent processing interval (CPI), and  $t_r$  is the pulse repetition interval (PRI). The required energy ratio  $D(1)$  for detection is the value for the single output of the coherent integrator. The result is a general radar equation (similar to that of Hall, discussed in Section

1.4.1), applicable to continuous-wave (CW) and pulsed Doppler radars as well as to noncoherent pulsed radars.

The application of the Blake chart to coherent radar requires merely the replacement of  $P_t$  with average power  $P_{av}$  in kW, and  $\tau$  with  $t_f$  in  $\mu\text{s}$ . If those units are inconvenient for CW radars, they may be replaced by watts and milliseconds without changing the range-equation constant.

Equation (1.18) is based on the assumption that detection is performed using the output of a Doppler filter without subsequent noncoherent integration. This limitation can be avoided, and the equation applied to radars using noncoherent integration of  $n'$  filter outputs, by replacing  $D(1)$  with  $D(n')$ . The increase in available energy, relative to (1.16), is expressed by the ratio  $P_{av}t_f/P_t\tau > 1$  in the numerator, and the decrease in required single-sample energy relative to (1.18) through the ratio  $D(n')/D(1) < 1$  in the denominator. The coherent and noncoherent gains from all  $n$  pulses are thereby included in the range calculation.

Blake's radar equation, promulgated also through the first two editions of Skolnik's *Radar Handbook* [15, 16], yields an accurate prediction of the maximum detection range for a target at any elevation angle, using realistic models of radars with any types of waveform and processing under actual environmental conditions. The steps required to modify his equations for modern radar problems are relatively minor, and are discussed in Section 1.6.

### 1.3.5 Blake's Bistatic Range Equation

Blake extends his basic radar equation to bistatic systems [12, Eq. (1.38)]:

$$\text{Bistatic radar: } (R_t R_r)_m^{1/2} = \left[ \frac{P_t \tau G_t G_r \lambda^2 \sigma_b F_t^2 F_r^2}{(4\pi)^3 k T_s D(n) C_b L} \right]^{1/4} \quad (\text{m}) \quad (1.19)$$

where  $R_t$  and  $R_r$  are the transmitter-to-target and target-to-receiver paths, respectively. The quantity  $(R_t R_r)^{1/2}$  is the geometric mean of the two paths in the bistatic system. The comments of Section 1.3.1 apply equally to this equation.

The Blake chart can also be used with bistatic radar, yielding the geometric mean range. Separate calculations of the pattern-propagation factors  $F_t$  and  $F_r$  are needed to arrive at the two-way factor  $F = (F_t F_r)^{1/2}$  in line 8 of the chart. The iteration procedures for attenuation in lines 9–14 are carried out using the sums of one-way attenuations over the two paths, considering their elevation angles (which should be recorded separately at the top of the chart along with the two antenna heights).

Blake's equations and chart are intended primarily for use in cases where targets are detected within the unambiguous range of the radar waveform. The results will be correct for detections beyond the unambiguous range, but errors may

arise from eclipsing by the transmission (see Section 1.6.1 and 10.1.2) or loss of integration caused by use of varying PRIs.

## 1.4 OTHER FORMS OF THE RADAR EQUATION

### 1.4.1 Hall's Radar Equations

Hall presents in [17] a radar equation for pulsed radar, preceding Blake's work, and clarifying many of the issues in previous literature:

$$\text{Pulsed radar: } R_m = \left[ \frac{P_t \tau G^2 \lambda^2 \sigma F^4}{(4\pi)^3 k T_0 F_n \times 1.2 D_x(n) L_t L_\alpha} \right]^{1/4} \quad (\text{m}) \quad (1.20)$$

This is equivalent to (1.14) with the following substitutions:

- The gain  $G^2$  for a common transmitting/receiving antenna replaces  $G_t G_r$ ;
- $F^4$  is included in the numerator as the two-way pattern-propagation factor;
- System temperature  $T_0 F_n$  is used for a receiver connected directly to the output terminal of an antenna in an environment at standard temperature  $T_0 = 290\text{K}$ ;
- The product  $1.2 D_x(n) L_t L_\alpha$ , replaces  $DL$ , where  $D_x(n)$  is the *effective detectability factor* given by the product of the following five terms:

$$\begin{aligned} D(n) &= \text{basic (theoretical) detectability factor for noncoherent integration of } n \text{ pulses;} \\ L_m &= \text{loss for nonoptimum bandwidth;} \\ L_p &= \text{beamshape loss;} \\ L_c &= \text{collapsing loss;} \\ L_o &= \text{operator and degradation factor.} \end{aligned}$$

The factor  $D_x$  is used in the equation for modern radars (see Section 1.6). The factor 1.2 that multiplies  $D_x$  in (1.20) represents the matching loss for an optimum receiver bandwidth  $B_n = 1.2/\tau$ , assuming an unmodulated pulse. Additional loss related to nonoptimum IF bandwidth is captured in the loss  $L_m$ .

A subsequent presentation by Hall of a general radar equation is applicable to monostatic and bistatic radars systems that use any waveform [18, Eq. (8)]:

$$\text{General case: } (R_t R_r)_m^{1/2} = \left[ \frac{P_{av} t_o G_t G_r \lambda^2 \sigma F_t^2 F_r^2}{(4\pi)^3 k T_s D_x(1) L_{at} L_{ar}} \right]^{1/4} \quad (\text{m}) \quad (1.21)$$

This expression combines Blake's (1.18) and (1.19), with the following substitutions:

- The coherent integration time  $t_f$  is assumed equal to the observation time  $t_o$ ;
- The product of detectability factor and loss  $D(1)L$  is replaced by  $D_x(1)L_{at}L_{ar}$ .
- The product of one-way atmospheric attenuations  $L_{at}$  and  $L_{ar}$  for the transmitting and receiving paths is used in the denominator.

Accurate results are available from Blake's widely promulgated method, so Hall's expressions have received little attention. They are included here to illustrate appropriate use of the energy ratio in radar equations.

#### 1.4.2 Barton's Radar Equations

The initial radar equation used in the 1964 *Radar System Analysis* [19] used peak transmitter power and noise power in the receiver bandwidth rather than energies. This lapse was corrected in the 1988 *Modern Radar System Analysis* [20] where radar equations are based on Blake's and Hall's work, the latter having introduced the *effective* detectability factor  $D_x(n)$  in place of the basic factor  $D(n)$  and its associated losses. Barton's equation for pulsed radar is [20, Eq. (1.2.25)]:

$$\text{Pulsed radar: } R_m = \left[ \frac{P_t \tau G_t G_r \lambda^2 \sigma F^4}{(4\pi)^3 k T_s D_x(n) L_t L_\alpha} \right]^{1/4} \quad (\text{m}) \quad (1.22)$$

The RF loss  $L_1$  that reduces available energy ratio are stated as separate terms  $L_t$  and  $L_\alpha$ . The loss  $L_2$  that increases the required energy ratio is included in  $D_x$ , and is defined to avoid error caused by use Blake's factor  $C_b$  in connection with electronic detection. Alternate forms of the equation are given for two types of coherent radar:

- Coherent integration over entire observation time [20, Eq. (1.2.26)], where energy  $P_{av} t_o$  in the observation time replaces single-pulse energy  $P_t \tau$ , and single-sample  $D_x(1)$  replaces  $D_x(n)$ ;
- Coherent integration over CPI, followed by noncoherent integration over  $t_o$  [20, Eq. (1.2.27)], where energy  $P_{av} t_f$  in the CPI replaces single-pulse energy  $P_t \tau$ , and  $D_x(n)$  is replaced by  $D_x(n')$ , where  $n' = t_o/t_f$ .

The second alternate form is used as the basis for a modified Blake chart, an example of which is shown in Figure 1.2.

**PULSE-RADAR RANGE-CALCULATION WORKSHEET**

The calculation is made for the parameters recorded in the two top lines of the chart.

1. **Compute** the system input noise temperature  $T_s$  following the outline in Part A.
2. **Enter** the range factors in basic units in Part B.
3. **Convert** these factors to decibel form and enter in Part C.

Detection probability $P_d$	<b>0.</b>	False-alarm probability $P_{fa}$	<b>10<sup>r</sup></b>	Target case:	.	Hits $n$	.		
Radar antenna height $h_r$ (m)			.	Target elevation angle $\theta^\circ$		.			
<b>A. Computation of <math>T_s</math>:</b>			<b>B. Range Factors</b>		<b>C. Decibel Values</b>		Plus	Minus	
$T_s = T_a + T_r + L_r T_e$			$P_t$ or $P_{av}$ (W)	.	$10 \log P$ (dBW)		.	.	
<b>(a)</b>	<b>Compute <math>T_a</math></b>		$\tau$ or $t_f$ (s)	.	$10 \log \tau$ (dBs)		.	.	
	For $T_{ig} = T_{ia} = 290\text{K}$ , $T_g = 36$ :		$G_t$	.	$G_t$ (dB)		.	.	
	$T_a = (0.876T_a' - 254)(1/L_a) + 290$		$G_r$	.	$G_r$ (dB)		.	.	
	$L_a$ (dB)	.	$L_a$ :	.	$\sigma$ (m <sup>2</sup> )		.	.	
			$T_a'$ (K)	.	$\lambda$ (m)		.	.	
		$T_a$ (K)	.	$T_e$ (K)		.	.		
<b>(b)</b>	<b>Compute <math>T_r = T_r(L_r - 1)</math></b>		$D$	.	$-D$ (dB)		.	.	
	$L_r$ (dB)	.	$L_r$ :	.	$M$		.	.	
	$T_r$	.	$T_r$ (K)	.	$L_p$		.	.	
<b>(c)</b>	<b>Compute <math>T_e = T_e(F_n - 1)</math></b>		$L_x$	.	$-L_x$ (dB)		.	.	
	$F_n$ (dB)	.	$F_n$ :	.	$L_t$		.	.	
	$T_e$ (K)	.	$L_r$ :	Range-equation constant $3.65 \times 10^7$ K/J				<b>+75.62</b>	.
			$L_r T_e$ (K)	<b>4. Obtain</b> column totals				.	.
<b>(d)</b>	<b>Add (a) + (b) + (c) = <math>T_s</math> (K)</b>		<b>5. Enter</b> the smaller total below the larger				.	.	
<b>6. Subtract</b> to obtain net decibels $X = 40 \log R_{0(\text{km})}$ (dBm <sup>4</sup> )									
<b>7. Calculate</b> $R_{0(\text{km})} = \text{antilog}(X/40)$							$R_{0(\text{km})}$	.	
<b>8. Calculate</b> the pattern-propagation factor $F = (F_t F_r)^{1/2}$							$F$	.	
<b>9. Multiply</b> $R_0$ by the pattern-propagation factor to obtain $R' = R_0 \times F$							$R'$	.	
<b>10. Determine</b> the atmospheric attenuation, loss $L_a$ (dB), corresponding to $R'$ . This is $L_a(\text{dB})_{(1)}$ .							$L_a(\text{dB})_{(1)}$	.	
<b>11. Find</b> the range factor $\delta_1 = \text{antilog}(-L_a(\text{dB})_{(1)}/40)$ .							$\delta_1$	.	
<b>12. Multiply</b> $R'$ by $\delta_1$ . This is a first approximation of range, $R_1$ .							$R_1$	.	
<b>13. If</b> $R_1$ differs appreciably from $R'$ , <b>find</b> a new value of $L_a$ (dB) corresponding to $R_1$ . This is $L_a(\text{dB})_{(2)}$ .							$L_a(\text{dB})_{(2)}$	.	
<b>14. Find</b> the range increase factor $\delta_2$ corresponding to the difference between $L_a(\text{dB})_{(1)}$ and $L_a(\text{dB})_{(2)}$ .							$\delta_2$	.	
<b>15. Multiply</b> $R_1$ by $\delta_2$ to obtain the maximum radar detection range $R_m$ in km							$R_m(\text{km})$	.	

Figure 1.2 Modified Blake chart [20, p. 21].

The user entries in this version of the Blake chart are in basic units, avoiding the multiple conversion factors of the original chart. The range-equation constant now includes only the factors  $(4\pi)^3$ ,  $k$ , and a factor converting range in m to km:

$$\begin{aligned} \text{Constant} &= \left[ (4\pi)^3 \cdot 1.38 \times 10^{-23} (\text{J/K}) (1000 \text{m/km})^4 \right]^{-1} \\ &= 3.65 \times 10^7 (\text{K} \cdot \text{km}^4 / \text{J} \cdot \text{m}^4) = 75.6 \text{ dB} \left[ \text{ref} (\text{K} \cdot \text{km}^4 / \text{J} \cdot \text{m}^4) \right] \end{aligned}$$

The procedures for entry, intermediate calculations, conversion to and from decibels, and iteration to account for atmospheric attenuation are the same as in the original Blake chart. Blake's  $C_b$  is replaced by the matching factor  $M$ , defined in Section 10.2.3.

The 2005 *Radar System Analysis and Modeling* gives the most general form of the radar equation as [21, Eq. (1.20)]:

$$\text{General case:} \quad R_m^4 = \frac{P_{av} t_f G_t G_r \lambda^2 \sigma F_p^2 F_t^2 F_r^2}{(4\pi)^3 k T_s D_x(n') L_t L_\alpha} \quad (\text{m}) \quad (1.23)$$

This is the form used for the modified Blake chart of Figure 1.2, but with an added factor  $F_p^2$  to account for possible polarization mismatch between transmitting and receiving antennas. That factor, normally set to unity, is included to emphasize the need to consider that the polarization of the receiving antenna may not match that applicable to the echo as calculated using the transmitted polarization and the normally specified target cross section  $\sigma$  in the radar equation. For example, when right-hand circular polarization is used both for transmission and reception, the usually specified  $\sigma$  gives the echo of the left-hand circular polarization component to which the receiving antenna is insensitive (see Section 10.1.1).

## 1.5 AVOIDING PITFALLS IN RANGE CALCULATION

It is appropriate here to comment on the different forms of the radar equation presented above and elsewhere in the literature, and to point out sources of error involved in their use.

### 1.5.1 System Noise Temperature $T_s$

The product  $kTF_n$  in the original equation (1.9) was intended to represent the noise spectral density  $N_0$  at the receiver input. Blake carefully defines his corresponding product  $kT_s$ , and its several components to improve the accuracy of noise calcula-

tions [12, p. 152]. His approach is especially important in modern systems where the noise figure is low and the antenna is directed toward the cold sky. His expressions are discussed in Chapter 6, with examples showing significant errors in results of the radar equation when the temperature of the environment that surrounds the radar is simply assumed to be  $T_0 = 290\text{K}$ .

Blake's formulation should be adopted as a permanent substitute for less meticulous expressions for thermal noise in any radar equation. This practice has been followed in the first two editions of Skolnik's *Radar Handbook* [15, 16] and in Barton [20–22]. Other presentations of the radar equation mistakenly rely on a simplified relationship  $N_0 = kT_0F_n$ , which is adequate only for radars in which  $F_n > 10$  dB. For modern radars it fails to model accurately the noise spectral density, with resulting errors in the order of 1–2 dB in calculation of the minimum required signal energy.

### 1.5.2 Use of Signal-to-Noise Energy Ratio

Both the original equation and those of Blake and Hall are properly based on ratios of input signal energy to noise spectral density, rather than of input power to noise power in some ill-defined (and generally unmeasurable) bandwidth. This allows the use of North's fundamental matched-filter relationship for the maximum available signal-to-noise ratio [3]:

$$\left(\frac{S}{N}\right)_{\max} = \frac{E}{N_0} \quad (1.24)$$

where  $E$  is signal energy and  $N_0$  the noise spectral density at the filter input. This gives the upper limit to potential radar performance, and can be applied to a radar using any waveform by applying a matching factor for cases in which the actual receiver and processor fall below the performance of the matched filter. The required input energy ratio is increased by this matching factor.

Radar equations using transmitter power  $P_t$  in the numerator and receiver bandwidth  $B_n$  or some "effective receiver bandwidth" in the denominator almost inevitably lead to errors, and are inapplicable when pulse compression or frequency-modulated CW signals are transmitted. Even with unmodulated pulses, when  $B_n < 1/\tau$ , the small value of  $B_n$  in the denominator of the equation leads to an erroneously large  $R_m$ , approaching infinity for  $B_n \rightarrow 0$  (which corresponds to an inoperative receiver). With  $B_n \gg 1/\tau$ , the resulting  $R_m$  may be too small because smaller video (or display) bandwidth reduces the noise relative to that passed by the receiver.

Surveying the radar literature, many authors place the noise power for receiver bandwidth  $B_n$  in the denominator of the radar equation. In cases where the pulse

energy does appear in the numerator, the derivation is often based on the assumption that an unmodulated pulse with  $B_n\tau = 1$  is used.

### 1.5.3 Use of Average Power

Radar equations that include average rather than peak transmitter power, such as (1.18), (1.21), or (1.23), are to be preferred because they emphasize the dependence of radar detection range in the thermal noise environment on average power, rather than on peak power or other waveform parameters. Those parameters are of practical importance for reasons other than establishing detection range. Use of peak power is not necessarily erroneous, as long as the contributions and losses from approximately matched filtering and integration, both coherent and noncoherent, are properly expressed for the waveform and processing actually used by the radar. Such expressions become increasingly difficult in modern radars, where system bandwidth is not a measureable parameter.

### 1.5.4 Bandwidth Correction and Matching Factors

An error arises when  $C_b$  expressed by (1.17) is applied in the equation for radars using electronic detection. The value  $C_b = 1.0$  for  $B_n\tau = 1.2$  falsely implies that such an “optimum filter” is a matched filter. The original radar equation was derived for radars with detection performed visually on a cathode-ray-tube display. The value of  $V$ , as determined experimentally, includes losses of 2–3 dB inherent in the display/observer process even when the “optimum bandwidth” is used [19, p. 171]. The detectability factor  $D$  used in (1.14) or (1.16) is defined for systems in which a matched filter is used, and hence requires use of a *matching factor*  $M$ , differing from  $C_b$ , to express any filter mismatch effects. This issue is discussed further in Sections 4.6 and 10.3.

### 1.5.5 Detectability Factors for Arbitrary Targets

Exact equations for detectability factors of commonly used target models are given in the literature and in Chapter 4. An expression for the single-pulse, steady target (Case 0) value denoted by  $D_0(1)$ , as derived by Rice [23], is readily solved using mathematical programs that run rapidly on personal computers. Marcum [24] extends the theory to  $D_0(n)$  for radars using noncoherent integration of multiple pulses. Swerling [25] gives expressions for detectability factors applicable to target models denoted by Cases 1–4 with amplitude statistics corresponding to chi-square distributions with two or four degrees of freedom and with slow or fast fluctuations of amplitude, denoted in this book by  $D_1(n)\dots D_4(n)$ . These exact expressions are supplemented in [21] by a generalized model leading to a factor  $D_e(n, n_e)$  for targets whose statistics follow the chi-square distribution with  $2n_e$

degrees of freedom. The generalized model covers Cases 0–4 and also targets for which the number of independent target samples is  $1 \leq n_e \leq n$ , including noninteger values commonly encountered.

Chapter 4 presents both exact and approximate methods of calculating detectability factors for all these models. Errors of several decibels can result from use of an inappropriate target system model, as is likely for targets described by Swerling models when the radar system takes advantage of diversity in time, frequency, space, or polarization.

### 1.5.6 Pattern-Propagation Factor

Inclusion of pattern-propagation factors  $F_i$  and  $F_r$ , or their geometric mean  $F$ , in the numerator of the radar equation is essential for accurate range calculation in any case where the target is not on the elevation beam axis and the elevation mainlobe is not clear of the surface underlying the radar-target path. Most texts contain some reference to the need for these factors, often discussing them separately from the radar equation, rather than embedding the factors in the equation. The treatment of this factor for phased array radars observing off-broadside targets requires special attention (see Section 10.2.1).

### 1.5.7 Loss Factors

The beamshape loss  $L_p$  is listed as one component of the loss factor  $L$  included in (1.16) and (1.18). This assumes that the target is not on the axis of the radar beam during the entire integration time of the echo pulses (e.g., when the radar scans across the target position). It is shown in Chapter 5 that  $L_p$  is a function of the required detection probability  $P_d$  unless several pulses, distributed across the mainlobe of the antenna pattern, are integrated as the beam scans.

Another issue that requires careful consideration is the relationship between beamshape loss and the antenna pattern embedded in the pattern-propagation factor  $F$ . Blake's method applies  $L_p$  to the effect of azimuth scan of a conventional 2-D search radar, while allowing  $F^4$  to describe the effect of the target position in the elevation pattern. For two-dimensional scan,  $F = 1$  can be used along with a loss  $L_p^2$  for regions where there are no surface-reflection effects and where the average performance over an elevation sector is to be evaluated. This issue will be discussed in Chapter 8.

In phased array radars, the gain at the beam axis varies with off-broadside scan angle. The gains  $G_i$  and  $G_r$  are normally defined on the beam axis at broadside, and the off-broadside scanning factor is included in the pattern-propagation  $F$ , which is then a function of both elevation and azimuth. Alternatively, an average scan loss over the sector may be defined (see Section 10.2.1) to account for the gain variation over the scan. As with beamshape loss, the scan sector loss in-

creases the energy ratio required at broadside by an amount that depends on the specified  $P_d$ , unless the energy transmitted in each beam dwell is adjusted as a function of scan angle to compensate for the reduced gain of the off-broadside beams (see Section 10.2.1).

The miscellaneous loss  $L_x$  in the equations is intended to include a number of loss factors, discussed in detail in Chapter 10. Several of these loss factors are also functions of the required  $P_d$ , and hence must be varied along with the detectability factor  $D$  if accurate range results are to be obtained.

### 1.5.8 Summary of Pitfalls in Range Calculation

Common errors in using the radar equation include the following:

- Use of  $T_0 = 290\text{K}$  rather than the actual system noise temperature  $T_s$ .
- Use of signal-to-noise power ratio in an ill-defined bandwidth  $B$ , instead of energy ratio. *Any radar equation that includes a receiver bandwidth  $B$  will cause confusion, at best, and at worst will cause serious errors in the range calculation.*
- Use of peak power without including the corresponding processing factors and losses.
- Use of the bandwidth correction factor  $C_b$  with other than the visibility factor  $V$  that includes the losses from visual detection.
- Use of a visibility factor or detectability factor that fails to account for statistics of the actual target and radar diversity.
- Failure to include the appropriate pattern-propagation factor.
- Failure to account for all the actual losses.

## 1.6 RADAR EQUATION FOR MODERN RADAR SYSTEMS

### 1.6.1 Factors Requiring Modifications to the Range Equation

Developments in radar technology and countermeasures to radar have imposed new problems in applying the radar range equation. Most of these problems can be solved by including an appropriate *range-dependent response factor*  $F_{\text{rdr}}$  in the numerator of the radar equation. The factor  $F_{\text{rdr}}$  includes several components as described below. The factors become especially important with low-observable targets, whose reduced cross sections may prevent detection beyond the range at which eclipsing and STC take effect.

### 1.6.1.1 Eclipsing

Eclipsing of the received signal occurs with two classes of waveform: (1) low-PRF radars using solid-state transmitters with duty cycles in excess of  $\approx 1\%$ ; and (2) medium- and high-PRF radars.<sup>5</sup>

- **Solid-State Transmitters.** Solid-state RF power amplifiers cannot provide high peak powers in exchange for low duty cycle<sup>6</sup>, as is the case for power tubes. Hence, the design of solid-state transmitters tends toward higher duty cycles, typically  $D_u = 5\%$  to  $20\%$ , in order to obtain the required average power while staying within the low peak rating of the devices. For low-PRF radar the pulse repetition interval  $t_r$  must be long enough to avoid range ambiguity, and higher  $D_u$  requires longer pulses than commonly used in tube transmitters. For example, an unambiguous range of 450 km requires  $t_r \geq 3$  ms. For  $D_u = 20\%$  the resulting transmitted pulsewidth  $\tau \geq 600$   $\mu$ s. Echoes from targets at range  $R < R_{\min} = \tau c/2 \approx 90$  km, are eclipsed: the early portions of the echo overlap the transmission, causing loss in signal-to-noise ratio. Echoes from  $R > R_u - R_{\min}$ , where  $R_u = c/2f_r$ , also suffer eclipsing of the far end of the echo. The radar equation for such cases includes a range-dependent *eclipsing factor*  $F_{\text{ecl}}$  as a component of  $F_{\text{rdr}}$ .

Some solid-state radars use dual-pulse groups in which each long pulse is accompanied by a shorter pulse, offset in frequency from the long pulse, to cover the short-range region eclipsed by the long pulse. In this case, only the average power of the longer pulse contributes to the detection of long-range targets, and the radar equation should reflect this. Eclipsing at the far end of the unambiguous range region is not avoided by using the short-range pulses.

The eclipsing factor for a radar that cannot detect a low-observable target beyond  $R_{\min}$  may prevent detection within that range.

- **MPRF and HPRF waveforms** have long been used in airborne radars, and appear also in some types of surface-based radar. Implicit in these waveforms is the requirement to detect targets with  $R > R_u$ . Calculation of maximum detection range then requires introduction of the eclipsing factor in the radar equation. The factor at a particular PRF is a deterministic function of range. When multiple PRFs are used in each beam position (either within the beam dwell or from scan to scan) the factor is usually represented statistically (see Section 10.2.1).

---

<sup>5</sup> The desired targets for low-PRF waveforms are within the unambiguous range; for high-PRF waveforms they are within the unambiguous velocity; for medium-PRF waveforms they are beyond both unambiguous range and velocity.

<sup>6</sup> Duty cycle (or duty factor) is the ratio of the pulse duration to the pulse repetition interval.

### 1.6.1.2 Sensitivity Time Control (STC)

Many low-PRF radars use STC to avoid saturation of the receiver or processor on large targets or clutter at medium and short range, and to suppress undesired detections of small moving objects such as birds and vehicle traffic at those ranges. STC is applied to reduce receive sensitivity at delays within some STC range  $R_{\text{stc}}$ , which is chosen to establish a threshold target cross section  $\sigma_{\text{min}}$  above which targets are to be detected. Attenuation is applied at RF prior to the receiver, or in the early stages of the receiver, to restrict the amplitude level of expected echo inputs. The effect of the range-dependent *STC factor*  $F_{\text{stc}}$  is illustrated below in Figure 1.5. A radar with STC loses the ability to detect, even at short range, a low-observable target whose cross section is less than  $\sigma_{\text{min}}$ .

### 1.6.1.3 Beam Dwell Factor

Radars may in some cases move the beam so rapidly that the receiving beam axis does not remain near the angle at which the transmitted pulse illuminates a long-range target, and from which the echo arrives after a delay  $t_d < t_r$ .

- If continuous scan occurs at a rate  $\omega$  such that the angular change  $\Delta\theta = \omega t_r$  between pulses is significant but less than the beamwidth in the scanned coordinate, a beam-dwell factor is introduced that depends on range. If  $\Delta\theta$  is greater than the beamwidth, the echo signal is lost.
- Radars with electronic scan usually scan in steps such that the beam dwells at the position used for transmission until the echo from the most distant expected target has arrived. In some cases, the receiving beam may return to the angle of a target that was illuminated by a prior pulse whose echo is sought, but that mode of operation is unusual, and the time available for the return dwell among other radar functions is limited.

In either case, the scanning radar discriminates against signals arriving with delay exceeding the dwell time of the beam in the direction of transmission, and a *beam dwell factor*  $F_{\text{bd}}$  is included as a component of  $F_{\text{rdr}}$  in the radar equation to describe this effect.

### 1.6.1.4 Frequency Agility or Diversity

Pulse-to-pulse change in frequency (agility) or group-to-group change (diversity) is used to evade jamming and to average the observed target RCS (e.g., for reduction in fluctuation loss). In either technique the receiver frequency is changed to that of the immediately preceding transmitted pulse. The beneficial effect on RCS averaging is included in the target model used to calculate the detectability factor  $D_e(n, n_e)$ . Discrimination against echo signals arriving after the frequency change

requires inclusion of a *frequency diversity factor*  $F_{fd}$  as a component of  $F_{rd}$  in the radar equation.

### 1.6.1.5 Lens Factor

The *lens loss* introduced by Weil [26] is caused by the change in tropospheric refraction with elevation angle. Although discussed by Blake [12, pp. 188–192], it is sometimes overlooked omitted because it does not appear as a specific term in the radar equation. To avoid this, the two-way *lens factor*  $F_{lens2}$  is included here as a component of  $F_{rd}$ . It must not be lumped with the atmospheric attenuation  $L_\alpha$  in the denominator of the equation because it is not a dissipative loss that increases the system noise temperature.

## 1.6.2 Equations Applicable to Modern Radars

*Modern Radar System Analysis Software, Version 3.0* [22] is a comprehensive set of worksheets (to be referred to as *MRSAS3*, and loosely termed a *program*), that runs under the Mathcad<sup>®</sup> program to calculate radar detection range and measurement accuracy. This version of program was developed during a period in which changes in radar technology and increased concern over reduction of target cross section exposed limitations in earlier forms of the radar equation, as discussed in Section 1.6.1. The program was designed to provide a more thorough analysis of radar performance, in which (1.23) was modified by addition of the range-dependent response factor  $F_{rd}$  for voltage response of the system, whose square modifies the *available* energy as a function of range:

$$E = \frac{P_{av} t_f G_t G_r \lambda^2 \sigma F_p^2 F_t^2 F_r^2 F_{rd}^2}{(4\pi)^3 R^4 L_\alpha} \quad (\text{J}) \quad (1.25)$$

where

- $F_{rd}$  =  $F_{ecl} F_{stc} F_{bd} F_{fd} F_{lens2}$  = product of radar response factors varying with range;
- $F_{ecl}$  = eclipsing factor;
- $F_{stc}$  = sensitivity-time-control factor;
- $F_{bd}$  = beam-dwell factor;
- $F_{fd}$  = frequency-diversity factor;
- $F_{lens2}$  = two-way lens factor.

These five factors are discussed in detail in Chapters 7 and 10, and for the present the following brief descriptions will suffice.

- *Eclipsing Factor.* Eclipsing has long been recognized as an important factor in high- and medium-PRF airborne radar, where the duty cycle exceeds that

commonly found in low-PRF systems. With the advent of high-duty-cycle, solid-state radar transmitters in surface-based radar, eclipsing becomes a more general problem. The resulting factor  $F_{\text{ecl}}$  is discussed in Section 10.1.2.

- *STC Factor.* STC applies a variable voltage gain  $F_{\text{stc}} \leq 1$  at RF prior to the receiver or in the early stages of the receiver (see Section 10.1.2). It is assumed here that significant competing noise is introduced in receiver stages subsequent to the STC, so that the output signal-to-noise ratio varies as the square of  $F_{\text{stc}}$ , compared to its value with constant gain.
- *Beam-Dwell Factor.* The beam-dwell factor  $F_{\text{bd}}$  is normally unity, but decreases when beam motion reduces the antenna gain on the target between the time the signal is transmitted and when the echo is received (see Section 10.1.2).
- *Frequency Diversity Factor.* The frequency diversity factor  $F_{\text{fd}}$  is unity as long as the receiver remains tuned to the frequency of the echo arriving at the radar. It is included here to ensure that echoes from ambiguous ranges are excluded, as dictated by use of frequency diversity or agility.
- *Lens Factor.* Weil showed that this factor reduces the available energy for targets near the horizon at long range, where the beam is spread in elevation by tropospheric refraction (see Section 7.4). Because it is not a dissipative loss that increases the antenna temperature, as does the atmospheric absorption loss  $L_{\alpha}$ , it is best expressed as a factor separate from absorption.

The resulting radar equation [22, Eq. (7.67)] is rewritten here to include the new range-dependent response factor:

$$\text{Modern radar: } R_m^4 = \frac{P_{\text{av}} t_f G_t G_r \lambda^2 \sigma F_p^2 F_t^2 F_r^2 F_{\text{rdr}}^2}{(4\pi)^3 k T_s D_x(n') L_t L_{\alpha}} \quad (\text{m}) \quad (1.26)$$

### 1.6.3 Method of Calculating Detection Range

A simple iteration procedure is used in the Blake chart to solve for detection range in the presence of range-dependent atmospheric attenuation. The introduction of the additional range-dependent response factors and the possible change in signal processing mode with range require a more robust method. This is based on the fundamental approach described in Section 1.1: the available and required energy ratios are found as functions of range, and the maximum range is found for which the two ratios are equal. The process can be graphical [21, Section 1.6], or implemented by computer [22]. Graphs generated as intermediate results in [22] illustrate that procedure and the effects of range-dependent terms on both available and required energy ratios.

## 1.6.3.1 Example Radar Range Calculation

Table 1.1 lists the parameters of a noncoherent 2-D low-altitude surveillance radar to be used as an example. The available and required energy ratios  $E/N_0$  and  $D_x$  for  $P_d = 50\%$  are shown in Figure 1.3, for a  $1.0\text{-m}^2$  target flying inbound at a constant  $1^\circ$  elevation, using *Modern Radar System Analysis Software* [22]. The program makes calculations at 100 equal inward steps in range, from a user-selected maximum (150 km in this case). To find  $R_m$ , values of  $E/N_0$  and  $D_x$  (in decibels) are inspected until their difference is positive. Interpolation is applied to find the exact

Table 1.1 Example 2-D Radar

Radar frequency $f_0$	3.0 GHz	Wavelength $\lambda$	0.10m
Peak power $P_t$	100 kW	Average power $P_{av}$	110.8W
Pulsewidth $\tau = \tau_n$	1.0 $\mu\text{s}$	Pulse repetition frequency $f_r$	1108 Hz
Transmitter line loss $L_t$	1.0 dB	Antenna gain $G$	40.0 dB
Azimuth beamwidth $\theta_a$	$1.3^\circ$	Elevation beamwidth $\theta_e$	$2.0^\circ$
Azimuth scan sector $A_m$	$360^\circ$	Frame time $t_s$	6.0
Pulses per dwell $n$	24	System temperature $T_s$	987K
Detection probability $P_d$	0.50	False-alarm probability $P_{fa}$	$10^{-6}$
Basic detectability factor $D$	2.7 dB	Matching factor $M$	0.8 dB
Beamshape loss $L_p$	1.2 dB	Miscellaneous loss $L_x$	3.3 dB
Detectability factor $D_x$	8.0 dB	Attenuation $L_\alpha$ (at $R_m$ )	1.8 dB
Pattern-propagation factor $F$	1.0	Range-dependent factor $F_{rdr}$	0 dB
Target RCS $\sigma$	$1.0\text{ m}^2$	Range in thermal noise $R_m$	132 km

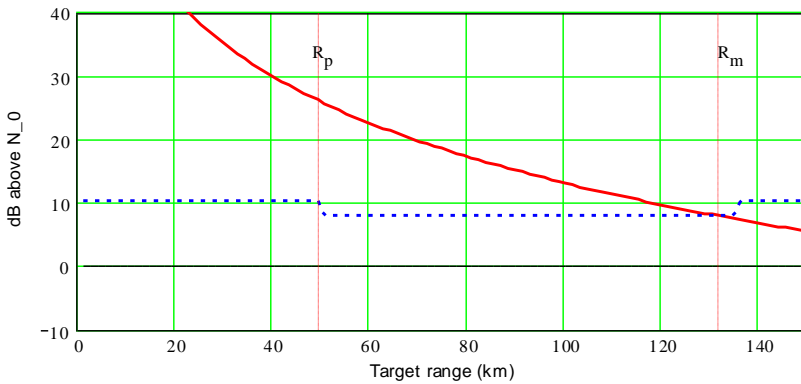


**Figure 1.3** Energy ratios versus range for example radar: signal energy (solid line), required energy (dashed line). MTI processing increases  $L_x$  for  $R < R_p = 50$  km.